Saudi Pharmaceutical Journal 30 (2022) 138–149

Contents lists available at ScienceDirect

Saudi Pharmaceutical Journal

journal homepage: www.sciencedirect.com

Original article

Metformin attenuates V-domain Ig suppressor of T-cell activation through the aryl hydrocarbon receptor pathway in Melanoma: In Vivo and In Vitro Studies

Fawaz E. Alanazi [a,d], Homood M. As Sobeai [a], Khalid Alhazzani [a], Abdullah Al-Dhfyan [b], Musaad A Alshammari [a], Moureq Alotaibi [a], Khaled Al-hosaini [a], Hesham M. Korashy [c], Ali Alhoshani [a,*]

[a] Department of Pharmacology & Toxicology, College of Pharmacy, King Saud University, P.O. Box 2457, Riyadh 11451, Saudi Arabia
[b] Stem Cell & Tissue Re-Engineering, King Faisal Specialist Hospital and Research Center, Riyadh 11211, Saudi Arabia
[c] Department of Pharmaceutical Sciences, College of Pharmacy, QU Health, Qatar University, Doha 2713, Qatar
[d] Pharmacy Services Department, Security Forces Hospital Program, P.O. Box 3643, Riyadh 11481, Saudi Arabia

ARTICLE INFO

Article history:
Received 15 October 2021
Accepted 27 December 2021
Available online 31 December 2021

Keywords:
VISTA
AHR
CYP1A1
IDO1
Metformin
CHL-1
B16
Melanoma

ABSTRACT

Melanoma is an aggressive skin cancer with a high rate of metastasis to other organs. Recent studies specified the overexpression of V-domain Ig suppressor of T-cell activation (VISTA) and Aryl Hydrocarbon Receptor (AHR) in melanoma. Metformin shows anti-tumor activities in several cancer types. However, the mechanism is unclear. This study aims to investigate the inhibitory effect of metformin on VISTA via AHR in melanoma cells (CHL-1, B16) and animal models. VISTA and AHR levels were assessed by qPCR, Western blot, immunofluorescence microscope, flow cytometry, and immunohistochemistry. Here, metformin significantly decreased VISTA and AHR levels in vitro and in vivo. Furthermore, metformin inhibited all AHR-regulated genes. VISTA levels were dramatically inhibited by AHR modulations using shRNA and αNF, confirming the central role of AHR in VISTA. Finally, melanoma cells were xenografted in C57BL/6 and nude mice. Metformin significantly reduced the tumor volume and growth rate. Likewise, VISTA and AHR-regulated protein levels were suppressed in both models. These findings demonstrate for the first time that VISTA is suppressed by metformin and identified a new regulatory mechanism through AHR. The data suggest that metformin could be a new potential therapeutic strategy to treat melanoma patients combined with targeted immune checkpoint inhibitors.

1. Introduction

Melanoma is caused by DNA mutations in melanocytes and is classified as an aggressive form of cancer with a high metastatic rate to other organs such as the brain, liver, and lungs (Patel et al., 1978, Balch et al., 2001). This deadly cancer has been rising for more than three decades due to poor prognosis in the early stage. Patients with stages I and II have almost five years to survive (98%), while stage IV metastatic melanoma has been shown only a 10% survival rate (Miller and Mihm 2006, Siegel et al., 2012, Heistein and Acharya 2018).

Metformin (1,1-dimethylbiguanide) is a widely prescribed first-line medication for patients with type two diabetes mellitus. Previous studies indicate that metformin decreases cancer incidence by 50% and inhibits cell proliferation in several cancers, including breast, melanoma, and pancreatic cancer (Cerezo et al., 2013, Tanaka et al., 2015, Zhang et al., 2017). Moreover, metformin exerts its anti-tumor effects by enhancing the cytotoxic T lymphocyte activity (CTL) in tumor tissues (Eikawa et al., 2015). These studies clearly demonstrate that metformin may have an anti-tumor functionality that enhances the activities of the immune response against tumor progression.

Sensitive interactions between immune checkpoint receptors and their ligands are critical to balance the activity of the immune system to avoid autoimmunity and tissue damage. Taking advantage of this system, cancer cells constitutively regulate checkpoint molecules to avoid immune system detection (Watanabe and

* Corresponding author at: Department of Pharmacology & Toxicology, College of Pharmacy, King Saud University, P.O. Box 2457, Riyadh 11451, Saudi Arabia.
E-mail address: ahoshani@ksu.edu.sa (A. Alhoshani).
Peer review under responsibility of King Saud University.

Production and hosting by Elsevier

https://doi.org/10.1016/j.jsps.2021.12.014
1319-0164/

Nakajima 2012). V-domain Ig suppressor of T cell activation, known as VISTA, is a negative checkpoint regulator. It is mainly expressed in hematopoietic cells, such as DCs, myeloid-derived suppressor cells (MDSCs), tumor-associated macrophages, and leukocytes such as naïve T cells (Lines et al., 2014a, 2014b). Moreover, VISTA is expressed in different cancer types such as breast cancer, epithelioid malignant pleural mesothelioma, and melanoma (Muller et al., 2020, Rosenbaum et al., 2020, Xie et al., 2020). VISTA can function as a receptor and a ligand. It has been found that VISTA acts as a receptor for the galectin-9 and VSIG-3 and as a ligand for PSGL-1 on tumors and T cells, respectively (Yum and Hong 2021). Thus, blocking or modulating VISTA's receptor-ligand interaction on immune and cancer cells may unleash T cell proliferation of tumor-antigen specific cells and attenuate MDSC's in the fight against tumor cells.

The aryl hydrocarbon receptor (AHR) is a ligand-activated transcription factor. Activation of the AHR/ARNT heterodimer complex by kynurenine produces a high expression of AHR-activity marker genes such as CYP1A1 (Matsumoto et al., 2007, Pollet et al., 2018, Lv et al., 2019). Several studies have demonstrated the involvement of AHR in cellular functions; cell cycle, cell differentiation, cell proliferation, cancer migration and progression, and apoptosis (Gramatzki et al., 2009, Dietrich and Kaina 2010, Kalmes et al., 2011, Maayah et al., 2015, Al-Dhfyan et al., 2017, Alhoshani et al., 2021). The AHR Antitumor immune responses modulate the AhR → IDO/TDO → AhR ligand amplification loop, and it consequently degrades tryptophan to produce AHR-ligand agonist (kynurenine and its metabolites). Kynurenine plays a role in the immune system, including T regulatory cell activation, and reduces the CTL activity (Puccetti and Grohmann 2007, Platten et al., 2012). Furthermore, kynurenine modulates PD-1 and PD-L1, raising the possibility that AHR contributes to immunosuppression via multiple checkpoint pathways (Liu et al., 2018, Wang et al., 2019). Previous studies (including our lab) have shown that metformin reduces CYP1A1 and CYP1B1 expression by down-regulating AHR signaling in breast cancer cells and inhibiting their growth (Do et al., 2014, Al-Dhfyan et al., 2017). Others have demonstrated that metformin acts as an adjuvant that can modulate the expression of negative immune checkpoint inhibitors (Liu et al., 2021). Thus, we hypothesized that metformin attenuates the VISTA immune checkpoint through AHR reduction. This study demonstrated that low metformin concentrations suppress VISTA expression through the AHR pathway in melanoma cells and animal models. Our findings with those supporting studies suggest that targeting both VISTA and AHR will provide efficient new approaches for metformin-based immunotherapy to promote the immune response and be essential with immunotherapy for melanoma treatment.

2. Methods

2.1. Cell culture and treatment

Human and mouse melanoma cell lines (CHL-1 and B16), obtained from American Type Culture Collection (Rockville, MD, USA), were maintained in Dulbecco's Modified Eagle Medium (DMEM) with 10% fetal bovine serum (FBS) and 1% of 100X Antibiotic-Antimycotic (ThermoFisher, USA). Cells were grown in 75- cm^2 tissue culture flasks at 37° C under a 5% CO_2 humidified environment. Cells were passaged 3–4 times before the first experiment and used below 10 passages. We treated CHL-1 and B16 cells with different concentrations of metformin. Prior to all experiments, we dissolved the stock solution of metformin in double-distilled water.

2.2. Cell viability and proliferation assay

The effect of metformin (Sigma-Aldrich Chemical Co., St. Louis, MO, USA) on cell viability was determined by the MTT assay (3-(4,5- dimethylthiazol-2-yl)-2,5-diphenyltetrazolium bromide), (ThermoFisher, Carlsbad, CA, USA), as previously described (Korashy and El-Kadi 2008). Cells were seeded at a density of 1×10^4 in 96-well plates and counted by LUNA-FI™ Dual Fluorescence Cell Counter (Logos Biosystems, Gyeonggi-do, South Korea) using 0.4% trypan blue (Fisher Scientific, Loughborough, UK). After 24 h, cells were treated with different metformin concentrations for 24 h (0–16 mM). Finally, cells were incubated with 1.2 μM of MTT reagent dissolved in phosphate buffer saline (PBS, pH 7.4) for 4 h at 37° C, then 100% isopropyl alcohol was added to dissolve formazan crystals for 15 min. The color intensity was measured at 570 nm by Mithras^2 LB 943 Microplate Reader (Berthold Technologies, Bad Wildbad, Germany). The percentage of cell viability was calculated relative to control (0 mM) designated as 100% viable cells using the following formula: % cell viability = (treated-background)/(control-background) × 100 (Thavornpradit et al., 2019). The percentage of cell viability was calculated by SigmaStat® for Windows, System Software Inc. (San Jose, CA, USA).

2.3. RNA extraction, cDNA synthesis, and quantification of mRNA expression by quantitative real time-polymerase chain reaction (qPCR)

Total cellular RNA was isolated from treated cells using TRIzol reagent as the manufacturer's recommendations (Invitrogen Co., San Diego, CA, USA). The quantity and quality were determined by measuring the 260/280 ratio (~2.0). cDNA synthesis was performed utilizing the High-Capacity cDNA reverse transcription kit (Applied Biosystems®, Foster City, CA, USA), according to the manufacturer's instructions as described previously (Korashy et al., 2012). Quantitative analysis of specific mRNA expression was performed by qPCR by subjecting the resulting cDNA products to PCR amplification using the QuantStudio 6 Flex System (Applied Biosystems®). The 20-μl reaction mixture contained forward and reverse primers, 10 μl of Fast SYBR Green Universal Master Mix (Applied Biosystems®), 8.8 μl of nuclease-free water, and 1 μl of cDNA sample. All primers were synthesized and purchased from Invitrogen (see Table 1). The changes in mRNA levels of the target gene relative to housekeeping genes were performed using the ΔΔ CT method as described previously (Livak and Schmittgen 2001).

2.4. Protein extraction and Western blot analysis

Total proteins were extracted from both melanoma cells treated with metformin as described before (Korashy and El-Kadi 2004). The protein concentrations were quantified using Direct Detect® Infrared Spectrometer, EMD Millipore Co. (Billerica, MA, USA). Western blot analysis was performed as described previously (Korashy and El-Kadi 2004). Briefly, 30 μg of protein from each group were separated in 10% sodium dodecyl sulfate-polyacrylamide gel electrophoresis (SDS-PAGE), then electrophoretically transferred into nitrocellulose membrane (0.45 μm). The protein blots were then incubated overnight at 4° C with blocking solution before incubation for 24 h with primary antibodies against target proteins and then peroxidase-conjugated secondary antibodies in blocking solution for 2 h at room temperature. The bands were visualized and then quantified by Image Lab 6.1 Software (Bio-Rad, Hercules, CA, USA) using the enhanced chemiluminescence method according to the manufacturer's instructions.

Table 1
Primers Sequences used for quantitative-PCR Reactions.

Gene	5′→3′ Forward primer	5′→3′ Reverse primer
Human VISTA	ACGCCGTATTCCCTGTATGTC	TTGTAGAAGGTCACATCGTGC
Human AHR	ACATCACCTACGCCAGTCGC	TCTATGCCGCTTGGAAGGAT
Human CYP1A1	CTATCTGGGCTGTGGGCAA	CTGGCTCAAGCACAACTTGG
Human IDO1	GCCTGATCTCATAGAGTCTGGC	TGCATCCCAGAACTAGACGTGC
Human β-ACTIN	TATTGGCAACGAGCGGTTCC	GGCATAGAGGTCTTTACGGATGTC
Mouse VISTA	GCATGGCGTCTAATGAGCAG	GGCAGAGGATTCCCACGATG
Mouse AHR	AGCCGGTGCAGAAAACAGTAA	AGGCGGTCTAACTCTGTGTTC
Mouse CYP1A1	GACCCTTACAAGTATTTGGTCGT	GGTATCCAGAGCCAGTAACCT
Mouse IDO1	GCAGACTGTGTCCTGGCAAACT	AGAGACGAGGAAGAAGCCCTTG
Mouse GAPDH	AGGTCGGTGTGAACGGATTTG	TGTAGACCATGTAGTTGAGGTCA

2.5. shRNA transfection

CHL-1 cells were seeded in six-well cell culture plates at a density of 2×10^5 cells per well for 24 h. Then, cells were transfected when the confluency reached 80% with four plasmids (ORIGENE, Rockville, MD, USA). Transfection was performed as described previously (Al-Dhfyan et al., 2017). Briefly, cells were seeded for 24 h, then media was changed to Opti-MEM medium (Sigma-Aldrich Chemical Co., St. Louis, MO, USA) and incubated at 37° C, shRNA vectors were mixed with Opti-MEM and Lipofectamine-2000 (Sigma-Aldrich Chemical Co.) and incubated for 30 min. Finally, the transfection mixture was added to each well and incubation for 6 h. Then, media was changed to complete media containing DMEM and 10% FBS without antibiotic for 24–48 h. Another 6-well cell culture plate containing CHL-1 cells was used to determine the concentration of puromycin for selection (Sigma-Aldrich Co.). Finally, cells were treated with puromycin (1 μg/ml) for 72 h, and the media was changed to complete media.

2.6. Confocal microscopy, data acquisition, and image analysis

CHL-1 and B16 cells were seeded at 5×10^4 cells in each well of the Ibidi® 8-well chamber slide (GmbH, Germany). After that, cells were treated with metformin (2, 4 mM for CHL-1 and 4, 8 mM for B16) then fixed with 4% paraformaldehyde (PFA-PBS). Fixed cells were incubated with 200 μl of PBS with tween-20 (PBST) overnight then, washed and incubated with the antibody for VISTA overnight (1 μl in 500 μl of 1% Bovine Serum Albumin, BSA, with PBST) then, secondary antibody conjugated with Alexa Flour-488 was added to each well for 1 h (2.5 μl in 500 μl of 1% BSA-PBST). Each sample was stained in triplicate. For the confocal setting, we followed the previously published study (Alshammari et al., 2016). Confocal images were acquired using the Zeiss LSM-800 confocal microscope with a Fluar (×5/0.25) objective, a Plan-Apochromat (×20/0.75na) objective, a C-Apochromat (×40/1.2 W Corr) objective, and Plan-Apochromat (×63/1.46 Oil) objective, with consistent gain and offset settings, and several confocal image Z-stacks across experimental sets. Multitrack acquisition was performed with an excitation line at 488 nm for Alexa 488. Z-series stack confocal images were taken at fixed intervals with the same pinhole setting; frame size was 1024 × 1024. All confocal images were analyzed using ImageJ software (http://imagej.nih.gov/ij). For VISTA expression levels, Z-stacks of confocal images were sum-projected, and a region of interest (ROI) corresponding to the cell was highlighted using an intensity threshold method and quantified was highlighted across the cell on VISTA staining's overlay image.

2.7. Flow cytometry

CHL-1 and B16 cells were treated with different metformin concentrations for 24 h, then incubated with rabbit anti-human against VISTA for 1 h on ice (1: 500, Sino Biological, China). Thereafter, a secondary antibody conjugated with Alexa Fluor-488 (1: 200, Santa Cruz, CA, USA) was added and incubated for 1 h on ice in the dark place. Each sample was stained in triplicate for VISTA antibody (Serke et al., 1998). The percentage of VISTA expression on the cell membrane was measured by Beckman Coulter flow cytometry.

2.8. Animal experiments, treatment, and calculations

All mice were provided by the Animal Care Center of the College of Pharmacy at King Saud University (KSU). They were housed in hygienic cages during the experiment (25° C with 12-hr dark/light cycle). Mice were randomly grouped and labeled as control, 100 mg and 200 mg. Melanoma cells were prepared in 100 μl of 1:1 of DMEM: Matrigel (Corning, NY, USA). On the 15th day, all mice were sacrificed under deep anesthesia (100 mg/kg ketamine and 10 mg/kg xylazine, intraperitoneally) (Xu et al., 2007).

Six to 8-week-old male nude and C57BL/6 mice were established by subcutaneously injecting 1×10^6 CHL-1 and 2×10^6 B16 cells, respectively, in the right flank region. Metformin (100 and 200 mg/kg) was intraperitoneally injected every other day from the fourth day of inoculation for two weeks, while the control group received normal saline (Herrera-Gayol and Jothy 2002). Finally, animals were sacrificed, and tumors were examined for VISTA and CYP1A1 expressions using the immunohistochemistry technique (Cha et al., 2018). We used this formula to calculate tumor volume: (length × width^2) × 0.52, and ln(V2/V1)/(T2 − T1) x100 to calculate the specific growth rate (SGR) (Bousquet et al., 1995, Mehrara et al., 2007). Where V is the tumor volume, and T represents the experimental period in days.

The animals were handled in accordance with the guide for Care and Use of Laboratory animals (Nih and Oer 2011), and the study protocol was approved by the Research Ethics Committee at the King Saud University (KSU-SE-20–62).

2.9. Immunohistochemistry staining assay

Immunohistochemistry (IHC) staining assay for VISTA and CYP1A1 expressions was performed using monoclonal mouse primary antibody for VISTA (Abcam, Cambridge, UK) and CYP1A1 (Thermo Fisher, Waltham, MA, USA). Tumors were fixed in 10% of formalin-PBS, and paraffin-embedded sections (3–5 μm) were subjected to IHC as described previously (Al-Dhfyan et al., 2017). Briefly, tumor paraffin sections were deparaffinized by two changes of xylene and rehydrated with descending grades of ethanol to distilled water. Sections were retrieved using 0.01 M citrate buffer (pH = 6) and exposed to irradiation in the microwave for 5 min. After washing by PBS, sections were blocked using 3% hydrogen peroxide for 10 min and then incubated with normal serum goat for 10 min after washing by PBS. Sections were incubated with primary antibody anti-VISTA (1:500) and anti-CYP1A1 (1:250) overnight at 4° C. Furthermore, sections were incubated with biotinylated secondary antibody for 30 min (abcam, Cambridge, UK), then avidin-biotin complex also for 30 min, followed

by chromogen (DAB) for 5 min kit, hematoxylin was used as a counterstain for 2 min. Sections were dehydrated, cleared, and covered. Sections were examined by light microscopy (Nikon-Japan) and photographed. Images were subjected to photo analysis by ImageJ software to obtain the percentage of anti-VISTA and anti-CYP1A1, counting of cells stained by DAB (N), and optical density (OD). The score was calculated according to N × OD/100 and classified as follows: negative is 0, weak is between 0 and 1, moderate is between 1 and 2, and more than 2 is strong (Volm et al., 1997).

2.10. Statistical analysis

The comparative analysis of the results from various experimental groups with their corresponding controls was performed using SigmaStat® for Windows (Systat Software, Inc, CA, USA). One-way analysis of variance (ANOVA) followed by Student–Newman–Keul's test or Student *t*-test was carried out to assess which treatment groups showed a significant difference from the control group. The differences will be considered significant when $p < 0.05$.

3. Results

3.1. Effect of metformin treatment on cell viability

First, we determined optimal concentrations of metformin by MTT assay in both CHL-1 and B16 cells. To evaluate this, we treated cells with a variety of metformin concentrations ranging 1–16 mM for 24 h. Results from low concentrations metformin treatment (1, 2, 4, and 8 mM) showed reduced cell viability by 15% in CHL-1 cells and 14.5% in B16 cells, with 80% of the cells remaining viable following treatment. Alternately, with high concentration treatment (10 and 16 mM), cell viability declined in CHL-1 cells, but the increase in concentration did not significantly reduce viability in B16 cells (Fig. 1). Drawing from these results, noncytotoxic concentrations of metformin (2, 4, and 8 mM) are ideal for use with CHL-1 cells. Low concentrations of metformin (4, 8, and 16 mM) with a noncytotoxic effect on cell viability are ideal for use with B16 cells. Based on these findings, these respective concentrations were used for all subsequent experiments.

3.2. Metformin treatment attenuates VISTA expression in melanoma cell lines

To assess the potential modulatory effect of metformin on VISTA levels in CHL-1 and B16 melanoma cells, we measured VISTA expression following metformin treatment using qPCR, Western blot analysis, immunofluorescence staining, and flow cytometry. Metformin treatment resulted in significant inhibition of VISTA mRNA and protein levels in CHL-1 and B16 cells. CHL-1 cells treated with 2, 4, and 8 mM of metformin showed decreased VISTA mRNA expression by 80, 93, and 92%, respectively, compared to the control (Fig. 2A). Similarly, B16 cells exposed to 4, 8, and 16 mM of metformin exhibited VISTA mRNA diminished by 74, 89, and 81%, respectively (Fig. 2B). Furthermore, we found that with the concentrations listed above, metformin downregulates VISTA proteins by up to 16, 22, and 29% in CHL-1 cells and 7, 54, and 67% in B16 cells (Fig. 2C, 2D).

To further delineate the effect of metformin on VISTA levels, we performed an immunofluorescence assay with confocal microscopy. We used lower concentrations of metformin in both cell lines (2, 4 mM in CHL-1 and 4, 8 mM in B16 cells). The results indicated a significant reduction in the fluorescence signals of VISTA in both CHL-1 and B16 cells (Fig. 3).

Previous studies demonstrate that VISTA engaged with T cells and other receptors to suppress the immune system activity and promote cancer (Le Mercier et al., 2014, Lines et al., 2014a, 2014b). To gauge the potential effect of metformin treatment on this interaction, we used flow cytometry to examine the VISTA levels on cell surfaces. CHL-1 cells treated with 2 and 4 mM of metformin for 24 h showed reduced surface VISTA levels by approximately 11 and 8%, respectively (Fig. 4A). In the same way, B16 cells exposed to 4 and 8 mM of metformin for 24 h exhibited downregulated surface VISTA levels by 7 and 14% (Fig. 4B). In combination, the aforementioned results indicate that VISTA mRNA and protein expression levels in CHL-1 and B16 cells are markedly attenuated by 24 h of metformin treatment.

3.3. Metformin represses the AHR pathway in melanoma cell lines

To determine whether metformin decreases the level of AHR and its regulated genes CYP1A1 and IDO1 in melanoma cells, we evaluated the expression levels by qPCR and Western blot analysis. First, we treated CHL-1 cells with metformin in concentrations of 2, 4, and 8 mM for 24 h, resulting in decreased AHR mRNA expressions by 31, 14, and 19%, respectively (Fig. 5A). Furthermore, expression of the AHR activity marker, CYP1A1, declined by 83, 95, and 94%, respectively (Fig. 5B), and IDO1 mRNA presence also declined by 89, 95, and 94% (Fig. 5C).

Similarly, we treated B16 cells with 4, 8, and 16 mM of metformin for 24 h, resulting in significantly decreased AHR mRNA

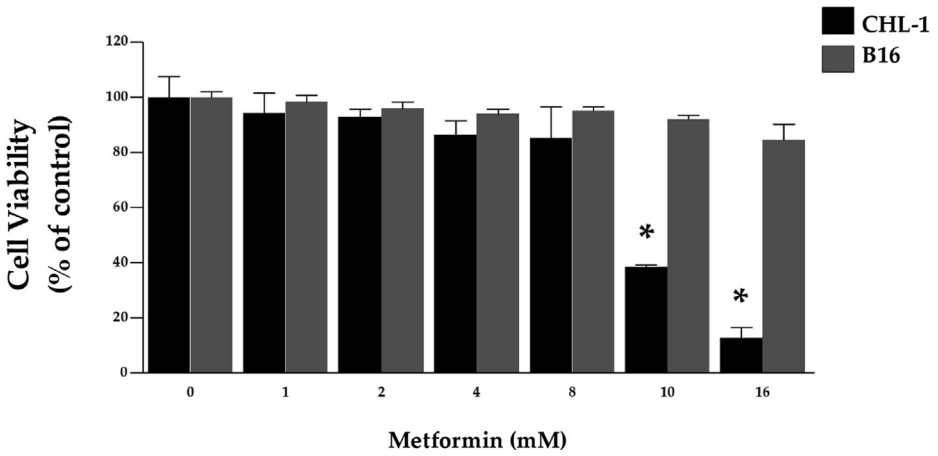

Fig. 1. Effect of metformin on cell viability. CHL-1 and B16 cells were treated with different metformin concentrations for 24 h (1–16 mM). Values are presented as a percentage of the control (mean ± SEM of three independent experiments). *Significantly different at $p < 0.05$ compared to the control (0 mM).

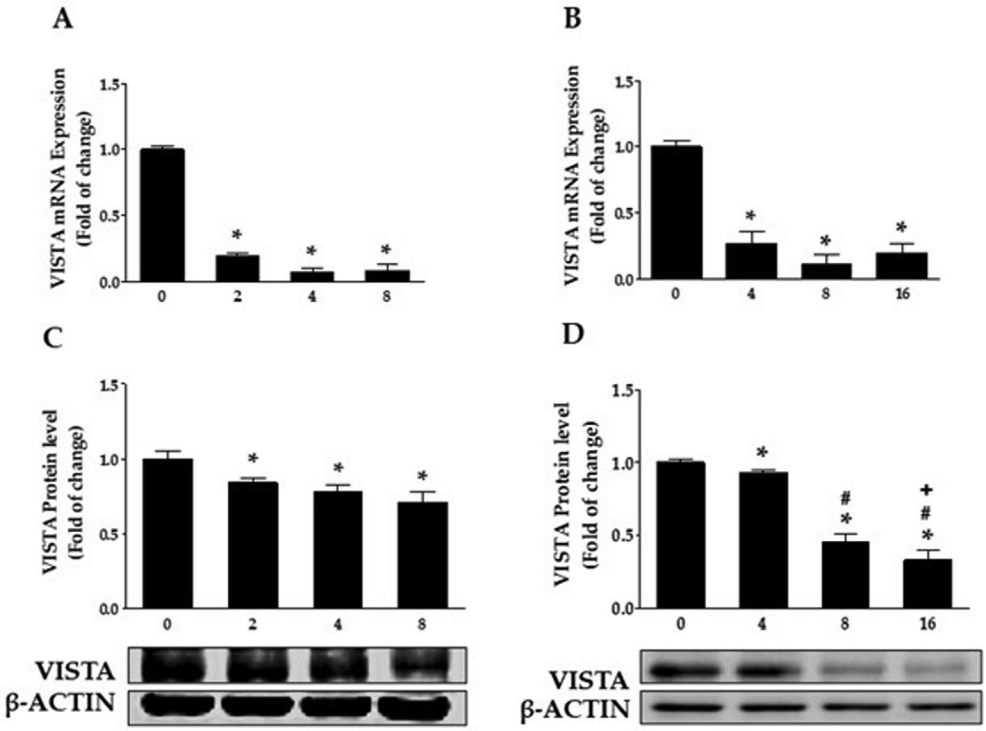

Fig. 2. Effect of metformin on VISTA expression. (A) mRNA level of VISTA in CHL-1 and (B) in B16 cells were measured by qPCR. Duplicate reactions were performed for each experiment, and the values represent the mean of fold change ± SEM, n = 6. *Significantly different at $p < 0.05$ compared to control (0 mM). Western blot analysis of VISTA protein in CHL-1 (C) and B16 cells (D). One of three representative experiments is shown. Values are presented as the mean ± SEM, n = 3, triplicate. *Indicates $p < 0.05$ statistically significant compared to the control (0 mM). #Indicates $p < 0.05$ statistically significant compared to 4 mM. +Indicates $p < 0.05$ statistically significant compared to 8 mM.

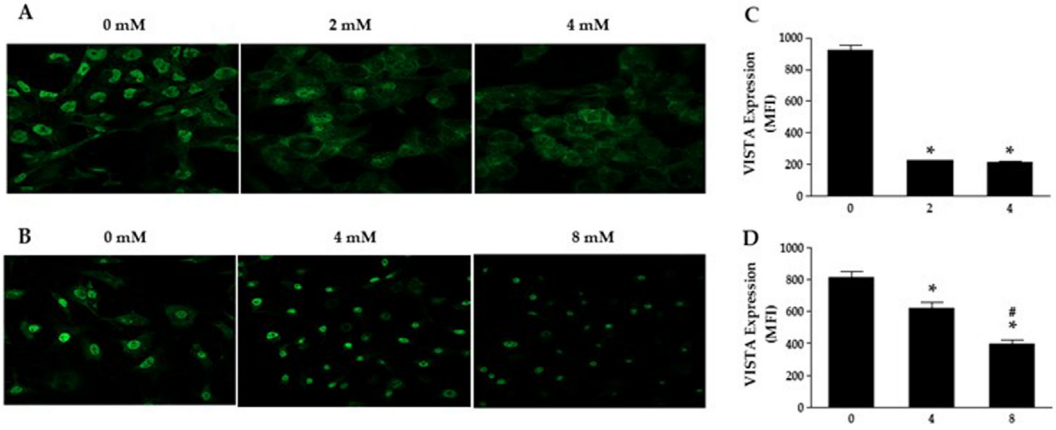

Fig. 3. Metformin decreases VISTA expressions. Representative confocal Z-stack images of the CHL-1 (A) and B16 cells (B) immunostained for VISTA (green). Total quantifications of VISTA expression in CHL-1 (C) and B16 cells (D). Confocal microscopy images, magnification 63X, bar: 50 μm. One of three representative experiments is shown. Triplicate reactions were performed for each experiment, and the values represent the mean ± SEM, n = 3. *Indicates $p < 0.05$ statistically significant compared to the control (0 mM).#Indicates $p < 0.05$ statistically significant compared to 4 mM.

expressions by 67, 83, and 73% (Fig. 5E). Additionally, expression of the AHR biomarker, CYP1A, declined by 81, 93, and 95% following 24 h metformin treatment (Fig. 5F). Under the same conditions, mRNA expression of IDO1 was downregulated by approximately 52, 68, and 68% (Fig. 5G). Of particular note among these results is that metformin strongly attenuated IDO1 gene expression in both cells, which is responsible for the induction of the AHR pathway due to its role in the degradation of tryptophan into kynurenine.

Additionally, we tested protein levels to confirm the effect of metformin on AHR and its regulated protein, CYP1A1, in melanoma cells. Consistent with our qPCR results, metformin at 2, 4, and 8 mM caused a significant decline in AHR protein levels by 25, 29, and 25% in CHL-1 cells. Metformin treatment also induced a reduction in CYP1A1 protein levels by 32, 48, and 53%, respectively (Fig. 5D). Likewise, B16 cells treated with 4, 8, and 16 mM of metformin led to 50, 55, and 59% decreases in AHR protein levels, and 7, 21, and 57% decrease in CYP1A1 protein levels (Fig. 5H). In conclusion, metformin treatment appears to induce the reduction of VISTA and AHR pathway expression levels, suggesting that the AHR pathway may be implicated in the regulation of VISTA levels in the tested cell lines.

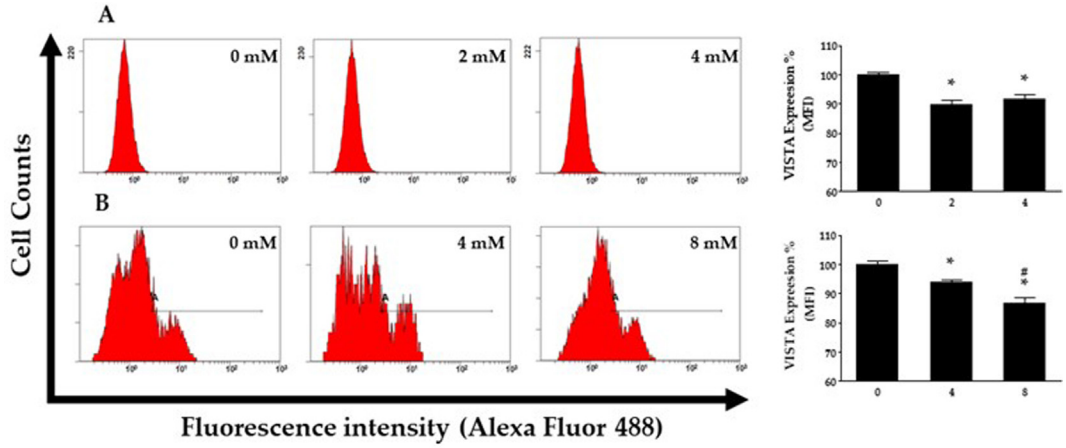

Fig. 4. Metformin reduces VISTA expression on the cell surface. CHL-1 (A) and B16 cells (B) were treated with metformin for 24 h. The percentage of VISTA expression on the cell surface was determined by flow cytometry as mean fluorescence intensity (MFI). One of three representative experiments is shown. Triplicate reactions were performed for each experiment, and the values represent the mean ± SEM, n = 3. *Indicates $p < 0.05$ statistically significant compared to the control (0 mM). #Indicates $p < 0.05$ statistically significant compared to 4 mM.

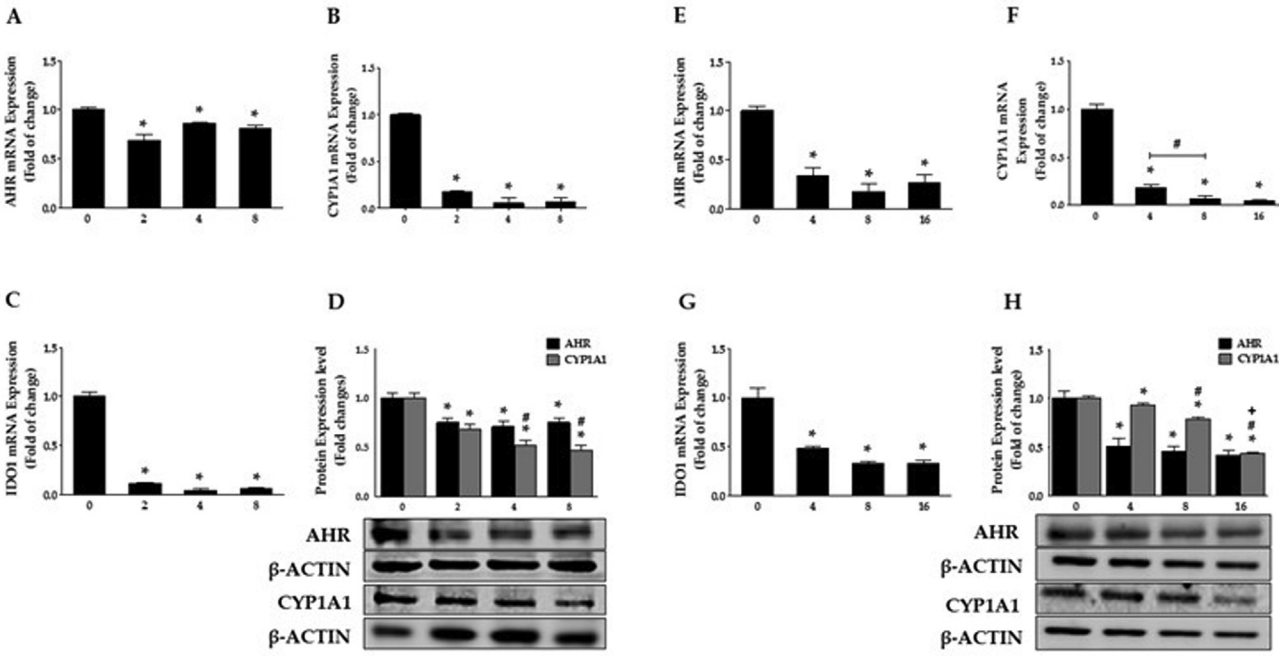

Fig. 5. Metformin represses the AHR/CYP1A1 pathway. The mRNA level of AHR, CYP1A1, and IDO1 in CHL-1 (A-C) and B16 (E-G) cells were quantified by qPCR. Duplicate reactions were performed for each experiment, and the values represent the mean of fold change ± SEM, n = 6. *Significantly different at $p < 0.05$ compared to the control (0 mM). AHR and CYP1A protein levels were determined by Western blot analysis in CHL-1 (D) and B16 cells (H). One of three representative experiments is shown. The values present the mean ± SEM (n = 3, triplicate). *Indicates $p < 0.05$ statistically significant compared to the control (0 mM). #Indicates $p < 0.05$ statistically significant compared to 2 mM in CHL-1 and 4 mM in B16 cells. +Indicates $p < 0.05$ statistically significant compared to 8 mM.

3.4. AHR pathway regulates VISTA expression level

Based on the findings detailed above, we proceeded to examine the involvement of AHR and CYP1A1 in regulating VISTA expression in melanoma cell lines by genetic and pharmacological approaches. First, we investigated whether the genetic knockdown of AHR would suppress the VISTA level. Two shRNA sequences were designed to knockdown the AHR gene in CHL-1 cells. Fig. 6 shows that AHR gene expression decreased by approximately 61 and 51%, respectively, compared to control shRNA. In addition, CYP1A1 decreased by up to 33 and 74%, respectively. Consistently, the inhibition of AHR/CYP1A1 was associated with downregulation of VISTA gene expression by approximately 31 and 27%, respectively. These results indicate a strong correlation between VISTA and the AHR /CYP1A1 pathway in melanoma.

In the second approach, we tested the pharmacological modulation of the AHR pathway level using Western blot. We used alpha-naphthoflavone (αNF) as an AHR stimulant or inhibitor, depending on the concentration (Blank et al., 1987, Santostefano et al., 1993, Lu et al., 1995, Zhou and Gasiewicz 2003). Two concentrations of αNF were treated CHL-1 for 24 h, and results showed that 5 μM significantly decreased VISTA, AHR, and CYP1A1 protein levels by up to 33, 30, and 24%, as compared to untreated cells. The concentration to induce AHR level (10 μM) resulted in a significant increase in VISTA (35%), AHR (59%), and CYP1A1 (42%) levels compared to untreated cells (Fig. 7A). In B16 cells, the lower concentrations of

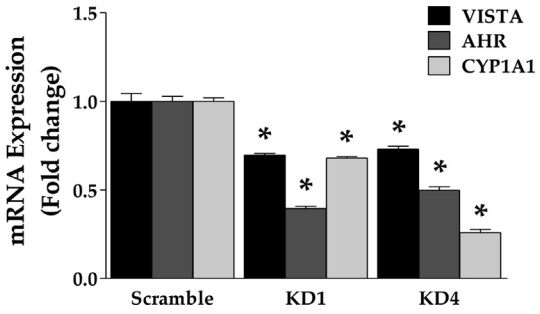

Fig. 6. The AHR pathway is essential for VISTA expression. CHL-1 cell was transfected with human AHR shRNA plasmids (1 and 4). The mRNA levels of VISTA, AHR, and CYP1A1 genes were quantified by qPCR. Duplicate reactions were performed for each experiment, and the values represent the mean of fold change ± SEM, n = 6. *Significantly different at $p < 0.05$ compared to the control shRNA.

αNF (2.5 and 5 μM) were used for 24 h. The protein levels of VISTA significantly decreased compared to control cells (approximately by 51 and 13%, respectively). AHR protein levels also decreased considerably by 11 and 22%, along with AHR-regulated proteins, which showed a significant reduction by 2.5 and 5 μM (by 30 and 54%, respectively). We observed that 10 μM αNF after 24 h of treatment significantly increased VISTA, AHR, and CYP1A1 protein levels by 32, 42, and 17%, respectively, compared to untreated cells (Fig. 7B). Taken together, these approaches identify the involvement of the AHR pathway in controlling VISTA expression levels in melanoma cells.

3.5. In vivo studies

3.5.1. Metformin treatment reduces melanoma growth

To examine the effect of metformin on melanoma animal models, we used nude and C57BL/6 mice. First, we inoculated the nude mice with CHL-1 cells and treated them with 100 and 200 mg/kg of metformin every other day for two weeks (Fig. 8A). Compared to untreated mice, six doses of metformin treatment induced a reduction in tumor volume by 81.8 and 73.8% (Fig. 8B) and lowered the growth rate by 64.5 and 69.6%, respectively (Fig. 8C). Second, B16 cells were inoculated in C57BL/6 mice and treated with metformin every 48 h for six doses within two weeks. We observed that metformin significantly reduced the tumor volume by 38.86 and 43.74%, respectively, compared to untreated mice (Fig. 8D). Additionally, the growth rate decreased by 25.8 and 36.7%, as well (Fig. 8E). These results strongly indicate the effectiveness of metformin on melanoma tumor tissues.

3.5.2. Metformin treatment reduces VISTA and CYP1A1 expression in melanoma animal models

In order to examine the effect of metformin on VISTA and CYP1A1 levels, the expression levels were determined by immunohistochemistry analysis. We treated melanoma tumors in nude mice with 100 mg/kg of metformin revealed moderate immune reactivity against anti-VISTA. The score was 1 compared to 2.6 in untreated mice and less VISTA percentage, 28% compared to 39% in untreated mice. Additionally, 200 mg/kg of metformin showed the most significant weak immune reactivity against VISTA associated with a lower percentage of anti-VISTA (score and percentage were 0.3 and 22%, respectively) (Fig. 9B, C). VISTA level in C57BL/6 mice treated with metformin (100 and 200 mg/kg) showed significant suppression, results represented as score (0.4 and 0.1, respectively, compared to 3 in untreated mice) and as a percentage (26 and 17%, respectively, compared to 56% in control mice) (Fig. 10B, C).

Immunohistochemical analysis showed a significant decrease in CYP1A1 expression levels compared to untreated tumors in nude mice (Fig. 11A). The anti-CYP1A1 score in tumors treated with 100 mg and 200 mg significantly decreased (0.2 and 0.07, respectively, compared to 2 in untreated mice) (Fig. 11B). Metformin treatment sharply reduced the CYP1A1 percentage (38 and 26% compared to 50% in untreated mice, respectively) (Fig. 11C). Finally, B16 cells were injected in C57BL/6 mice and treated with metformin (100 and 200 mg/kg). Results showed that metformin significantly decreased CYP1A1 levels (Fig. 12A). Anti-CYP1A1 scores were 0.2 and 0.09, respectively, compared to 1 in untreated mice (Fig. 12B). The percentage showed a significant decrease (38.77 and 61.22%, respectively) (Fig. 12C). These results strongly indicate the effect of metformin on tumor growth and VISTA/CYP1A1 expression levels in vivo melanoma models.

4. Discussion

Developing a new therapeutic strategy to address cancer, and melanoma, in particular, is a crucial challenge. Current studies

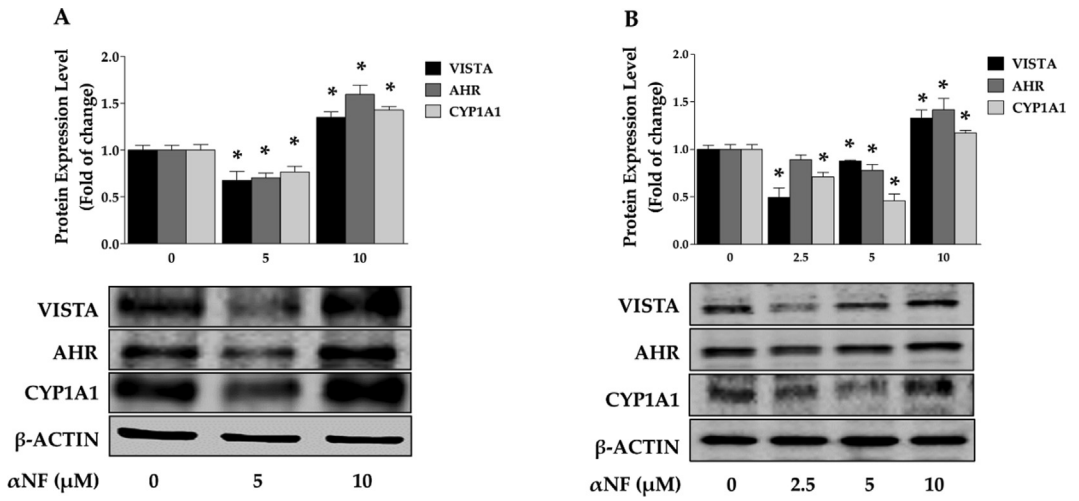

Fig. 7. AHR modulator influences VISTA level. The protein expression levels of VISTA, AHR, and CYP1A1 were determined by Western blot analysis in CHL-1 (A) and B16 (B) cells. One of three representative experiments is shown. Values are presented as the mean ± SEM, n = 3, triplicate. *Significantly different at $p < 0.05$ compared to the control (αNF 0 μM).

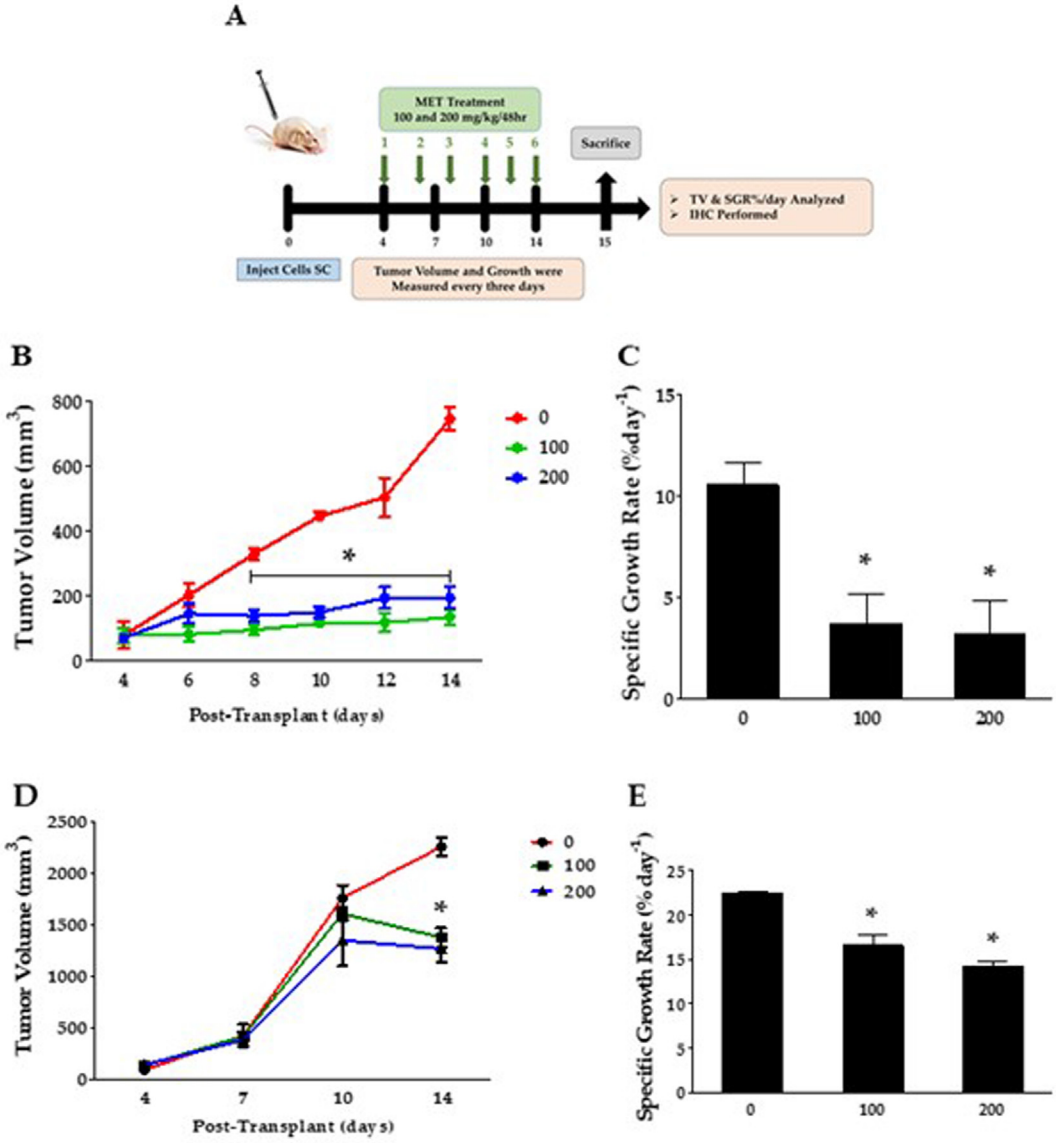

Fig. 8. Metformin reduces tumor growth in mice models. (A) The experimental scheme for metformin treatment and the tumor growth and volume were measured two times per week. (B) The tumor volume of nude mice were injected with 1×10^6 CHL-1 cells and treated with metformin every other day for 14 days. (C) Average specific growth rate % per day (SGR%/day) of CHL-1 cells in different groups. (D) Tumor volume of C57BL/6 mice were injected with 2×10^6 B16 cells. (E) Average specific growth rate % per day of B16 cells in different groups. Values are means ± SEM. *Statistical significance is indicated when $p < 0.05$ compared to untreated mice.

have shown that in patients diagnosed with melanoma, there was an overexpression of VISTA as well as AHR. A high expression level of VISTA has been reported in patients with low survival rates and worse progression. Moreover, VISTA is critically associated with other immune checkpoint expressions, such as PD-1, by up to 30% in melanoma patients (Choi et al., 2020). Therefore, metformin was hypothesized to have an inhibitory effect on VISTA via the AHR in the CHL-1, B16 cell lines, and animal models. Both VISTA and AHR expression levels, along with regulated genes, were assessed utilizing qPCR, Western blot, flow cytometry, immunofluorescence microscopy, and immunohistochemistry.

The present study demonstrates that the lower concentrations of metformin repress VISTA expression through the AHR pathway. Mechanistically, metformin acts as an inducer of energetic stress in cancer cells, mainly through activating the AMPK-driven signaling pathway (Ras-MAPK and PI3K-AKT/mTOR), which was thought to be essential for the anti-mitotic activity (Huang et al., 2008, Kalender et al., 2010, Hajjar et al., 2013, Pernicova and Korbonits 2014). Another study showed that metformin inhibited breast cancer through the AHR pathway (Maayah et al., 2015, Alhoshani et al., 2021). In addition, metformin was evaluated when given in combination with immune checkpoint inhibitors (anti-PD-1/anti-CTLA-4) in patients who had been diagnosed with metastatic melanoma. The results indicate a favorable response in this patient population (Afzal et al., 2018).

The results presented in this study focus on the inhibitory effect of metformin on VISTA expression levels and the regulatory role of the AHR pathway in melanoma. We observed that metformin suppressed VISTA and AHR/CYP1A1 family at gene and protein expression levels. AHR and CYP1A1 family expressions are consistent with the results of DO MT, Wang GZ, and Kim Y et al. (Do et al., 2014, Maayah et al., 2015, Wang et al., 2019, Alhoshani et al., 2021, Kim et al., 2021). Also, recent studies demonstrated that metformin enhanced immunity by several approaches (Scharping et al., 2017, Afzal et al., 2018, Cha et al., 2018, Bahrambeigi and Shafiei-Irannejad 2020).

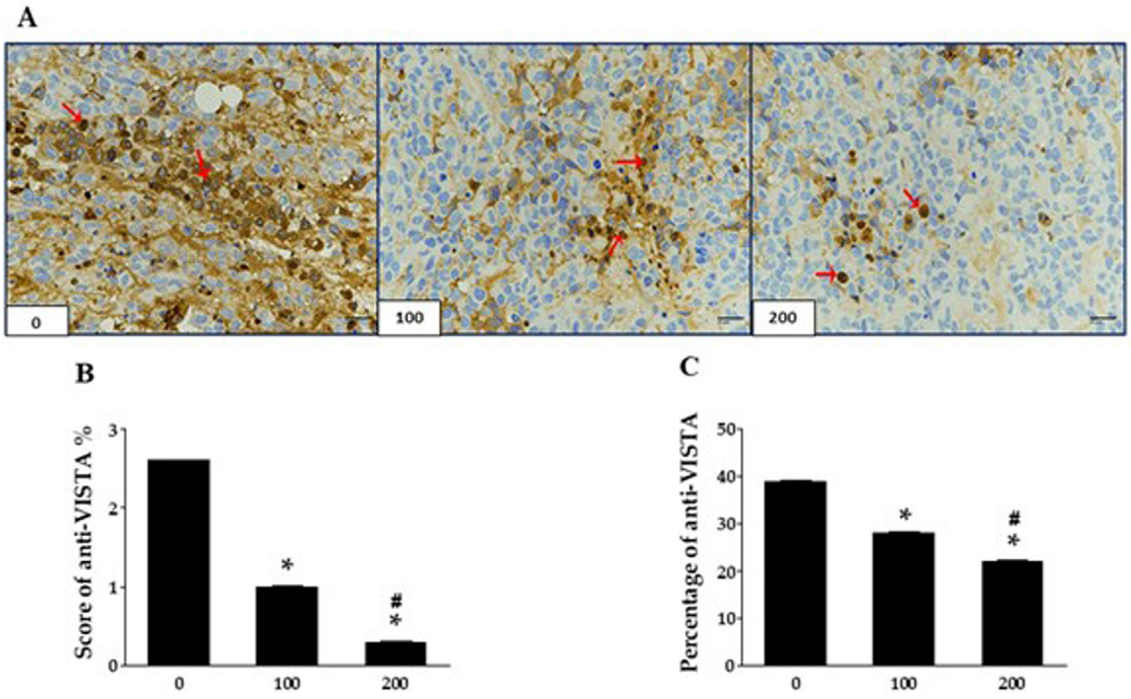

Fig. 9. Metformin suppresses VISTA expression in nude mice. Mice were injected with 1×10^6 CHL-1 cells treated every other day for 14 days. Tumors were tested immunohistochemically against anti-VISTA, (A) untreated control tumor, 100 mg, and tumor treated with 200 mg/kg of metformin. The red arrows indicate VISTA-positive expression, and size bars are 25 μm. IHC was performed using an Avidin-Biotin Complex Method, Original magnifications 400-fold. (B) Scoring of immune reactivity against anti-VISTA. (C) Percentage of anti-VISTA. Values are means ± SEM. *Indicates $p < 0.05$ statistically significant compared to untreated mice. #Indicates $p < 0.05$ statistically significant compared to mice treated with 100 mg/kg.

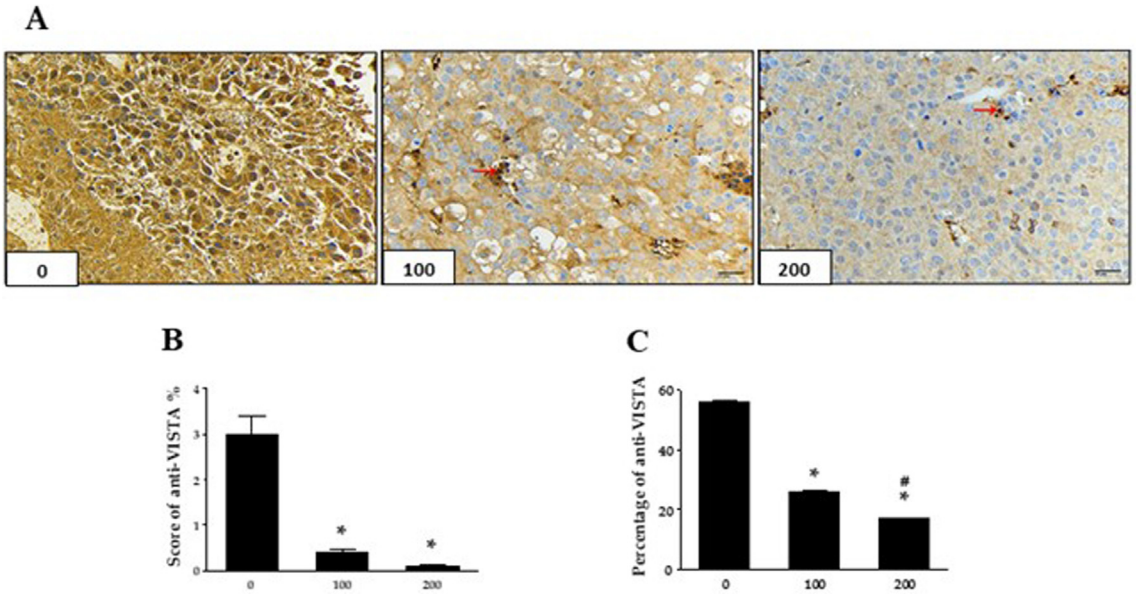

Fig. 10. Metformin attenuates VISTA expression in C57BL/6 mice. Mice were injected with 2×10^6 B16 cells divided into three groups and treated every other day with metformin for two weeks. Tumors were tested immunohistochemically against anti-VISTA, (A) untreated control tumor, 100 and 200 mg/kg of metformin. The red arrows indicate VISTA-positive expression, and size bars are 25 μm. IHC was performed using an Avidin-Biotin Complex Method, Original magnifications 400-fold. (B) The scoring of immune reactivity against anti-VISTA, (C) The percentage level of anti-VISTA. Values are means ± SEM. *Indicates $p < 0.05$ statistically significant compared to untreated mice. #Indicates $p < 0.05$ statistically significant compared to mice treated with 100 mg/kg.

Furthermore, the IDO1 expression is essential for the AHR pathway. Our findings show that the metformin significantly inhibited IDO1 expression, contributing to the down-regulation of AHR, CYP1A1, and VISTA gene expression levels. The IDO1-TDO-KYN-AHR pathway expression has been studied in different tumor samples. Opitz et al. have shown that IDO1 and TDO are essential for the KYN level, subsequently activating the AHR pathway (Opitz et al., 2011, Pilotte et al., 2012). Up to now, five ongoing studies targeting IDO in clinical trials. Therefore, this study suggests that metformin could induce novel synergistic effects with IDO inhibitors. Further investigation to explore the regulatory effect of the AHR pathway on VISTA expression using AHR-shRNA gene knockdown,

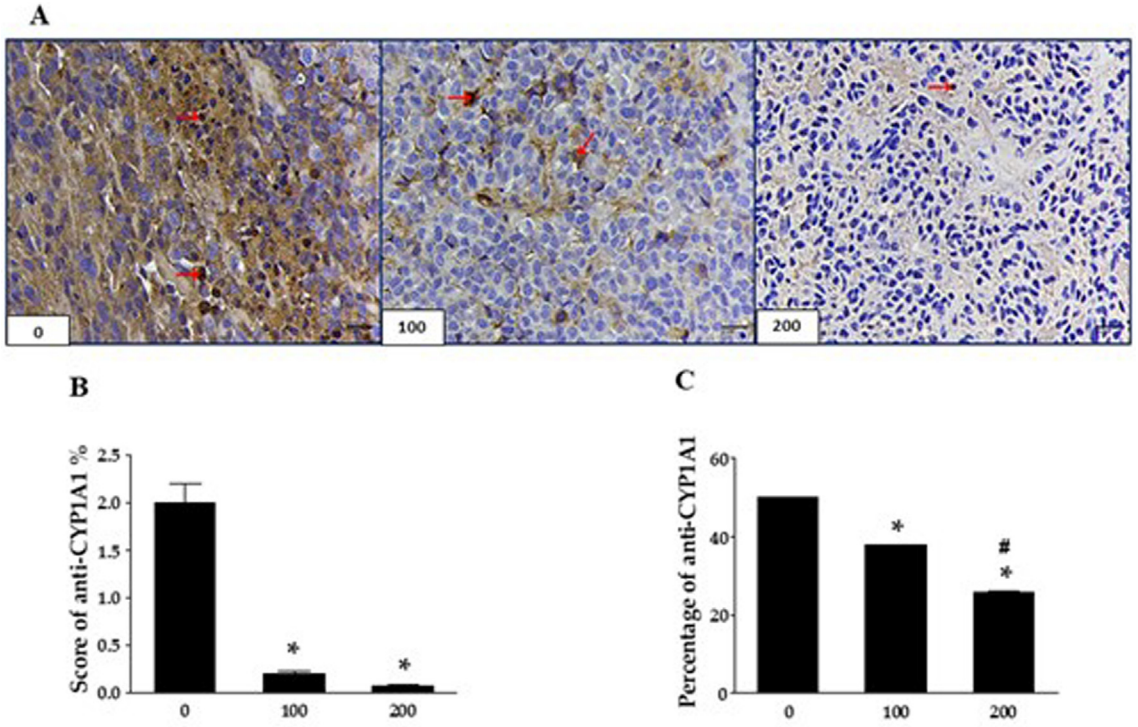

Fig. 11. Metformin suppresses CYP1A1 expression in nude mice. Mice were injected with 1×10^6 CHL-1 cells divided into three groups and treated with metformin every other day for 14 days. Tumors were tested immunohistochemically against anti-VISTA, (A) 0, 100, and 200 mg/kg of metformin. The red arrows indicate CYP1A1-positive expression, and size bars are 25 μm. IHC was performed using an Avidin-Biotin Complex Method, Original magnifications 400-fold. (B) The scoring of immune reactivity against anti- CYP1A1, (C) the percentage level of anti-CYP1A1. Values are means ± SEM. *Indicates $p < 0.05$ statistically significant compared to untreated mice. #Indicates $p < 0.05$ statistically significant compared to mice treated with 100 mg/kg.

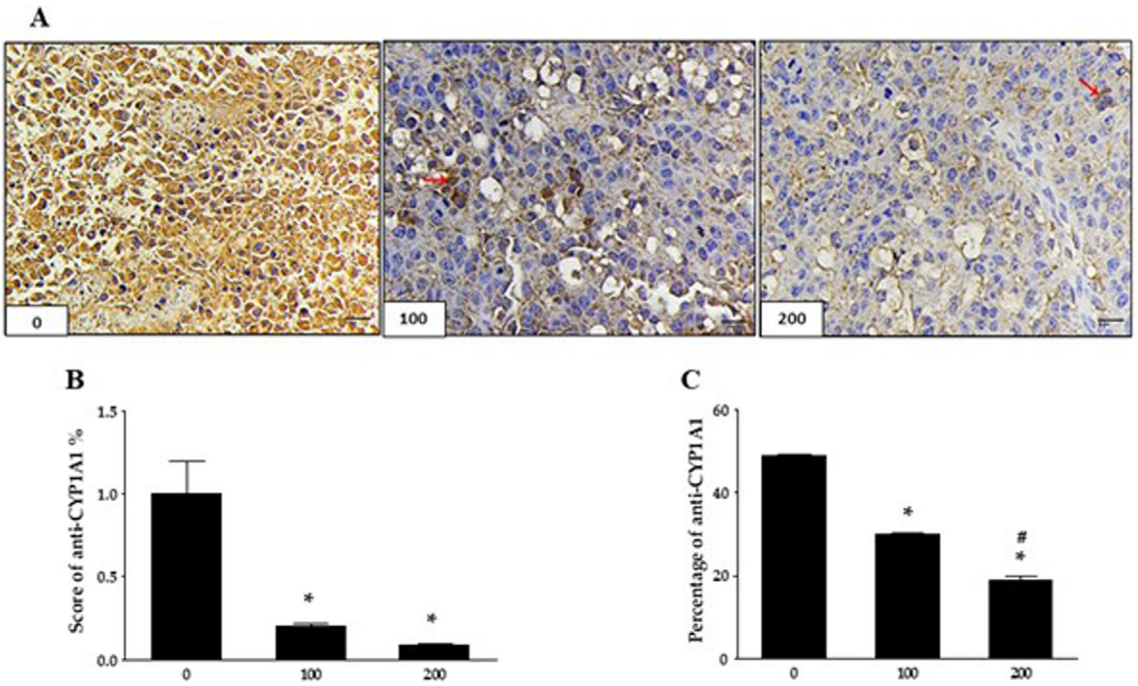

Fig. 12. Metformin inhibits the expression of CYP1A1 in C57BL/6 mice. C57BL/6 mice were injected with 2×10^6 B16 cells divided into three groups (0, 100, and 200 mg/kg/dose of metformin). Tumors were tested immunohistochemically against anti-CYP1A1, (A) tumor treated with 0, 100, and 200 mg/kg of metformin. (B) The scoring of immune reactivity against anti-CYP1A1 and (C) represents the percentage level of anti-CYP1A1. The red arrows indicate CYP1A1-positive expression, and size bars are 25 μm. IHC was performed using an Avidin-Biotin Complex Method, Original magnifications 400-fold. Values are means ± SEM. *Indicates $p < 0.05$ statistically significant compared to untreated mice. #Indicates $p < 0.05$ statistically significant compared to mice treated with 100 mg/kg.

we found that the AHR pathway is crucial in the regulation of VISTA expression in melanoma cells. However, we cannot exclude the chemical modulator of the AHR pathway in this study. Therefore, we used different concentrations of αNF in both melanoma cells by taking the advantages of αNF on the AHR pathway as a stimulant or inhibitor depending on the concentration (Santostefano et al., 1993, Murray et al., 2011). The inhibition of AHR by αNF has been investigated by Wang GZ et al., they reported that αNF in combination with anti-PD-L1 decreased the tumor growth and potentiated the cell infiltration associated with a significant increase in TNFα and INFγ expression levels (Wang et al., 2019).

From in vitro experiments, we explored the effect of metformin in human and mouse melanoma cells to confirm the role of the AHR pathway on VISTA expression. These findings suggest that targeting VISTA and the AHR pathway by metformin combined with an immunotherapeutic agent such as anti-PD-1 or anti-CTLA-4 might be more convenient for patients suffering from deadly metastatic melanoma.

The next step in our study was to evaluate these results in vivo. The melanoma cell lines CHL-1 and B16 were xenografts in nude and C57BL/6 mice, respectively. The results indicated that the tumor volume and growth rate within the nude and C57BL/6 mice were significantly impaired compared to the control. In addition, both VISTA and AHR-regulated protein, CYP1A1, expression levels were reduced.

In conclusion, metformin suppresses the expression of VISTA in a new regulatory mechanism through AHR at in vivo and in vitro levels, which elucidates the nature of the relationship between AHR and VISTA. This study indicates that there is great promise that metformin combined with immune checkpoint inhibitors could potentially be a treatment for patients who have been diagnosed with melanoma.

Declaration of Competing Interest

The authors declare that they have no known competing financial interests or personal relationships that could have appeared to influence the work reported in this paper.

Acknowledgement

The authors would like to thank Deanship of scientific research in King Saud University for funding and supporting this research through the initiative of DSR Graduate Students Research Support (GSR).

References

Afzal, M.Z., Mercado, R.R., Shirai, K., 2018. Efficacy of metformin in combination with immune checkpoint inhibitors (anti-PD-1/anti-CTLA-4) in metastatic malignant melanoma. J. Immunother. Cancer 6 (1). https://doi.org/10.1186/s40425-018-0375-1.

Al-Dhfyan, A., Alhoshani, A., Korashy, H.M., 2017. Aryl hydrocarbon receptor/cytochrome P450 1A1 pathway mediates breast cancer stem cells expansion through PTEN inhibition and β-Catenin and Akt activation. Mol. Cancer.

Alhoshani, A., Alotaibi, M., As Sobeai, H.M., Alharbi, N., Alhazzani, K., Al-Dhfyan, A., Alanazi, F.E., Korashy, H.M., 2021. In Vivo and In Vitro Studies Evaluating the Chemopreventive Effect of Metformin on the Aryl Hydrocarbon Receptor-Mediated Breast Carcinogenesis. Saudi J. Biol. Sci. 28 (12), 7396–7403.

Alshammari, M.A., Alshammari, T.K., Nenov, M.N., Scala, F., Laezza, F., 2016. Fibroblast growth factor 14 modulates the neurogenesis of granule neurons in the adult dentate gyrus. Molecular 53 (10), 7254–7270.

Bahrambeigi, S., Shafiei-Irannejad, V., 2020. Immune-mediated anti-tumor effects of metformin; targeting metabolic reprogramming of T cells as a new possible mechanism for anti-cancer effects of metformin. Biochemical 174, 113787. https://doi.org/10.1016/j.bcp.2019.113787.

Balch, C.M., Buzaid, A.C., Soong, S.-J., Atkins, M.B., Cascinelli, N., Coit, D.G., Fleming, I. D., Gershenwald, J.E., Houghton, A., Kirkwood, J.M., McMasters, K.M., Mihm, M. F., Morton, D.L., Reintgen, D.S., Ross, M.I., Sober, A., Thompson, J.A., Thompson, J. F., 2001. Final version of the American Joint Committee on Cancer staging system for cutaneous melanoma. J. Clin. Oncol. 19 (16), 3635–3648.

Blank, J., Tucker, A., Sweatlock, J., et al., 1987. alpha-Naphthoflavone antagonism of 2, 3, 7, 8-tetrachlorodibenzo-p-dioxin-induced murine lymphocyte ethoxyresorufin-O-deethylase activity and immunosuppression. Mol. Pharmacol.

Bousquet, P.F., Braña, M.F., Conlon, D., et al., 1995. Preclinical evaluation of LU 79553: a novel bis-naphthalimide with potent antitumor activity. Cancer Res.

Cerezo, M., Tichet, M., Abbe, P., Ohanna, M., Lehraiki, A., Rouaud, F., Allegra, M., Giacchero, D., Bahadoran, P., Bertolotto, C., Tartare-Deckert, S., Ballotti, R., Rocchi, S., 2013. Metformin blocks melanoma invasion and metastasis development in AMPK/p53-dependent manner. Mol. Cancer Ther. 12 (8), 1605–1615. https://doi.org/10.1158/1535-7163.MCT-12-1226-T.

Cha, J.-H., Yang, W.-H., Xia, W., Wei, Y., Chan, L.-C., Lim, S.-O., Li, C.-W., Kim, T., Chang, S.-S., Lee, H.-H., Hsu, J.L., Wang, H.-L., Kuo, C.-W., Chang, W.-C., Hadad, S., Purdie, C.A., McCoy, A.M., Cai, S., Tu, Y., Litton, J.K., Mittendorf, E.A., Moulder, S. L., Symmans, W.F., Thompson, A.M., Piwnica-Worms, H., Chen, C.-H., Khoo, K.-H., Hung, M.-C., 2018. Metformin promotes antitumor immunity via endoplasmic-reticulum-associated degradation of PD-L1. Mol. Cell 71 (4), 606–620.e7.

Choi, J.W., Kim, Y.J., Yun, K.A., Won, C.H., Lee, M.W., Choi, J.H., Chang, S.E., Lee, W.J., 2020. The prognostic significance of VISTA and CD33-positive myeloid cells in cutaneous melanoma and their relationship with PD-1 expression. Sci. Rep. 10 (1). https://doi.org/10.1038/s41598-020-71216-2.

Dietrich, C., Kaina, B., 2010. The aryl hydrocarbon receptor (AhR) in the regulation of cell–cell contact and tumor growth. Carcinogenesis 31 (8), 1319–1328.

Do, M.T., Kim, H.G., Tran, T.T.P., Khanal, T., Choi, J.H., Chung, Y.C., Jeong, T.C., Jeong, H.G., 2014. Metformin suppresses CYP1A1 and CYP1B1 expression in breast cancer cells by down-regulating aryl hydrocarbon receptor expression. Toxicol. Appl. Pharmacol. 280 (1), 138–148. https://doi.org/10.1016/j.taap.2014.07.021.

Eikawa, S., Nishida, M., Mizukami, S., Yamazaki, C., Nakayama, E., Udono, H., 2015. Immune-mediated antitumor effect by type 2 diabetes drug, metformin. Proc. Natl. Acad. Sci. USA 112 (6), 1809–1814. https://doi.org/10.1073/pnas.1417636112.

Gramatzki, D., Pantazis, G., Schittenhelm, J., Tabatabai, G., Köhle, C., Wick, W., Schwarz, M., Weller, M., Tritschler, I., 2009. Aryl hydrocarbon receptor inhibition downregulates the TGF-β/Smad pathway in human glioblastoma cells. Oncogene 28 (28), 2593–2605.

Hajjar, J., Habra, M.A., Naing, A., 2013. Metformin: an old drug with new potential. Expert Opin. Invest. Drugs 22 (12), 1511–1517.

Heistein, J. B. and U. Acharya, 2018. Cancer, Malignant Melanoma.

Herrera-Gayol, A., Jothy, S., 2002. Effect of hyaluronan on xenotransplanted breast cancer. Exper. Mol. Pathol.

Huang, X.u., Wullschleger, S., Shpiro, N., McGuire, V., Sakamoto, K., Woods, Y., Mcburnie, W., Fleming, S., Alessi, D., 2008. Important role of the LKB1–AMPK pathway in suppressing tumorigenesis in PTEN-deficient mice. Biochem. J. 412 (2), 211–221.

Kalender, A., Selvaraj, A., Kim, S.Y., Gulati, P., Brûlé, S., Viollet, B., Kemp, B.E., Bardeesy, N., Dennis, P., Schlager, J.J., Marette, A., Kozma, S.C., Thomas, G., 2010. Metformin, independent of AMPK, inhibits mTORC1 in a rag GTPase-dependent manner. Cell Metab. 11 (5), 390–401.

Kalmes, M., Hennen, J., Clemens, J., et al., 2011. Impact of aryl hydrocarbon receptor (AhR) knockdown on cell cycle progression in human HaCaT keratinocytes.

Kim, Y., Vagia, E., Viveiros, P., et al., 2021. Overcoming acquired resistance to PD-1 inhibitor with the addition of metformin in small cell lung cancer (SCLC). Cancer Immunol., Immunother.

Korashy, H.M., El-Kadi, A.O.S., 2004. Differential effects of mercury, lead and copper on the constitutive and inducible expression of aryl hydrocarbon receptor (AHR)-regulated genes in cultured hepatoma Hepa 1c1c7 cells. Toxicology 201 (1-3), 153–172.

Korashy, H.M., El-Kadi, A.O.S., 2008. Modulation of TCDD-mediated induction of cytochrome P450 1A1 by mercury, lead, and copper in human HepG2 cell line. Toxicology 22 (1), 154–158.

Korashy, H.M., Maayah, Z.H., Abd-Allah, A.R., El-Kadi, A.O.S., Alhaider, A.A., 2012. Camel milk triggers apoptotic signaling pathways in human hepatoma HepG2 and breast cancer MCF7 cell lines through transcriptional mechanism. J. Biomed. Biotechnol. 2012, 1–9. https://doi.org/10.1155/2012/593195.

Le Mercier, I., Chen, W., Lines, J.L., Day, M., Li, J., Sergent, P., Noelle, R.J., Wang, L.i., 2014. VISTA regulates the development of protective antitumor immunity. Cancer Res. 74 (7), 1933–1944.

Lines, J.L., Pantazi, E., Mak, J., Sempere, L.F., Wang, L.i., O'Connell, S., Ceeraz, S., Suriawinata, A.A., Yan, S., Ernstoff, M.S., Noelle, R., 2014a. VISTA is an immune checkpoint molecule for human T cells. Cancer Res. 74 (7), 1924–1932.

Lines, J.L., Sempere, L.F., Broughton, T., Wang, L.i., Noelle, R., 2014b. VISTA Is a Novel Broad-Spectrum Negative Checkpoint Regulator for Cancer Immunotherapy. Cancer Immunol. Res. 2 (6), 510–517.

Liu, W., Wang, Y., Luo, J., Liu, M., Luo, Z., 2021. Pleiotropic Effects of Metformin on the Antitumor Efficiency of Immune Checkpoint Inhibitors. Frontiers 11. https://doi.org/10.3389/fimmu.2020.586760.

Liu, Y., Liang, X., Dong, W., Fang, Y.i., Lv, J., Zhang, T., Fiskesund, R., Xie, J., Liu, J., Yin, X., Jin, X., Chen, D., Tang, K.e., Ma, J., Zhang, H., Yu, J., Yan, J., Liang, H., Mo, S., Cheng, F., Zhou, Y., Zhang, H., Wang, J., Li, J., Chen, Y., Cui, B., Hu, Z.-W., Cao, X., Xiao-Feng Qin, F., Huang, B.o., 2018. Tumor-Repopulating Cells Induce PD-1

Expression in CD8+ T Cells by Transferring Kynurenine and AhR Activation. Cancer Cell 33 (3), 480–494.e7.
Livak, K.J., Schmittgen, T.D., 2001. Analysis of relative gene expression data using real-time quantitative PCR and the 2(-Delta Delta C(T)) Method. Methods. S1046-2023(01)91262-9 [pii].
Lu, Y.F., Santostefano, M., Cunningham, B.D.M., Threadgill, M.D., Safe, S., 1995. Identification of 3′-methoxy-4′-nitroflavone as a pure aryl hydrocarbon (Ah) receptor antagonist and evidence for more than one form of the nuclear Ah receptor in MCF-7 human breast cancer cells. Arch. Biochem. Biophys. 316 (1), 470–477.
Lv, J.-W., Zheng, Z.-Q., Wang, Z.-X., Zhou, G.-Q., Chen, L., Mao, Y.-P., Lin, A.-H., Reiter, R.J., Ma, J., Chen, Y.-P., Sun, Y., 2019. Pan-cancer genomic analyses reveal prognostic and immunogenic features of the tumor melatonergic microenvironment across 14 solid cancer types. J. Pineal Res. 66 (3), e12557. https://doi.org/10.1111/jpi.2019.66.issue-310.1111/jpi.12557.
Maayah, Z.H., Ghebeh, H., Alhaider, A.A., El-Kadi, A.O.S., Soshilov, A.A., Denison, M.S., Ansari, M.A., Korashy, H.M., 2015. Metformin inhibits 7, 12-dimethylbenz [a] anthracene-induced breast carcinogenesis and adduct formation in human breast cells by inhibiting the cytochrome P4501A1/aryl hydrocarbon receptor signaling pathway. Toxicol. Appl. 284 (2), 217–226.
Matsumoto, Y., Ide, F., Kishi, R., Akutagawa, T., Sakai, S., Nakamura, M., Ishikawa, T., Fujii-Kuriyama, Y., Nakatsuru, Y., 2007. Aryl Hydrocarbon Receptor Plays a Significant Role in Mediating Airborne Particulate-Induced Carcinogenesis in Mice. Environ. Sci. Technol. 41 (10), 3775–3780.
Mehrara, E., Forssell-Aronsson, E., Ahlman, H., Bernhardt, P., 2007. Specific growth rate versus doubling time for quantitative characterization of tumor growth rate. Cancer Res. 67 (8), 3970–3975.
Miller, A.J., Mihm, M.C., 2006. Melanoma. N. Engl. J. Med. 355 (1), 51–65. https://doi.org/10.1056/NEJMra052166.
Muller, S., Victoria Lai, W., Adusumilli, P.S., Desmeules, P., Frosina, D., Jungbluth, A., Ni, A.i., Eguchi, T., Travis, W.D., Ladanyi, M., Zauderer, M.G., Sauter, J.L., 2020. V-domain Ig-containing suppressor of T-cell activation (VISTA), a potentially targetable immune checkpoint molecule, is highly expressed in epithelioid malignant pleural mesothelioma. Mod. Pathol. 33 (2), 303–311.
Murray, I.A., Flaveny, C.A., Chiaro, C.R., Sharma, A.K., Tanos, R.S., Schroeder, J.C., Amin, S.G., Bisson, W.H., Kolluri, S.K., Perdew, G.H., 2011. Suppression of cytokine-mediated complement factor gene expression through selective activation of the Ah receptor with 3′, 4′-dimethoxy-α-naphthoflavone. Molecular 79 (3), 508–519.
Nih, O., Oer, O., 2011. Guide laboratory animals for the care and use of. Committee for the Update of the Guide for the Care and Use of Laboratory Animals Institute for Laboratory Animal Research Division on Earth and Life Studies. The National Academies Press Washington, DC, USA.
Opitz, C.A., Litzenburger, U.M., Sahm, F., et al., 2011. An endogenous tumour-promoting ligand of the human aryl hydrocarbon receptor. Nature.
Patel, J., Didolkar, M., Pickren, J., et al., 1978. Metastatic pattern of malignant melanoma: a study of 216 autopsy cases. Am. J. Surg.
Pernicova, I., Korbonits, M., 2014. Metformin—mode of action and clinical implications for diabetes and cancer. Nat. Rev. Endocrinol.
Pilotte, L., Larrieu, P., Stroobant, V., et al., 2012. Reversal of tumoral immune resistance by inhibition of tryptophan 2, 3-dioxygenase. Proc. Natl. Acad. Sci.
Platten, M., Litzenburger, U., Wick, W., 2012. The aryl hydrocarbon receptor in tumor immunity. Oncoimmunology. https://doi.org/10.4161/onci.19071.
Pollet, M., Shaik, S., Mescher, M., et al., 2018. The AHR represses nucleotide excision repair and apoptosis and contributes to UV-induced skin carcinogenesis. Cell Death & Different.
Puccetti, P., Grohmann, U., 2007. IDO and regulatory T cells: a role for reverse signalling and non-canonical NF-kappaB activation. Nat. Rev. Immunol. https://doi.org/10.1038/nri2163.
Rosenbaum, S.R., Knecht, M., Mollaee, M., et al., 2020. FOXD3 regulates VISTA expression in melanoma. Cell reports.
Santostefano, M., Merchant, M., Arellano, L., et al., 1993. alpha-Naphthoflavone-induced CYP1A1 gene expression and cytosolic aryl hydrocarbon receptor transformation. Mol. Pharmacol.
Scharping, N.E., Menk, A.V., Whetstone, R.D., et al., 2017. Efficacy of PD-1 blockade is potentiated by metformin-induced reduction of tumor hypoxia. Cancer Immunol. Res.
Serke, S., van Lessen, A., Huhn, D., 1998. Quantitative fluorescence flow cytometry: a comparison of the three techniques for direct and indirect immunofluorescence. Cytometry.
Siegel, R., DeSantis, C., Virgo, K., et al., 2012. Cancer treatment and survivorship statistics, 2012. CA Cancer J. Clin. https://doi.org/10.3322/caac.21149.
Tanaka, R., Tomosugi, M., Horinaka, M., et al., 2015. Metformin Causes G1-Phase Arrest via Down-Regulation of MiR-221 and Enhances TRAIL Sensitivity through DR5 Up-Regulation in Pancreatic Cancer Cells. PLoS ONE. https://doi.org/10.1371/journal.pone.0125779.
Thavornpradit, S., Usama, S.M., Park, G.K., et al., 2019. QuatCy: a heptamethine cyanine modification with improved characteristics. Theranostics.
Volm, M., Koomägi, R., Mattern, J., 1997. Prognostic value of vascular endothelial growth factor and its receptor Flt-1 in squamous cell lung cancer. Int. J. Cancer.
Wang, G.-Z., Zhang, L., Zhao, X.-C., et al., 2019. The Aryl hydrocarbon receptor mediates tobacco-induced PD-L1 expression and is associated with response to immunotherapy. Nat. Commun.
Watanabe, N., Nakajima, H., 2012. Coinhibitory molecules in autoimmune diseases. Clin. Develop. Immunol.
Xie, X., Zhang, J., Shi, Z., et al., 2020. The Expression Pattern and Clinical Significance of the Immune Checkpoint Regulator VISTA in Human Breast Cancer. Frontiers. in immunology.
Xu, Q., Ming, Z., Dart, A.M., et al., 2007. Optimizing dosage of ketamine and xylazine in murine echocardiography. Clin. Exp. Pharmacol. Physiol.
Yum, J.I., Hong, Y.K., 2021. Terminating Cancer by Blocking VISTA as a Novel Immunotherapy: Hasta la vista, baby. Front Oncol. https://doi.org/10.3389/fonc.2021.658488.
Zhang, J., Li, G., Chen, Y., et al., 2017. Metformin Inhibits Tumorigenesis and Tumor Growth of Breast Cancer Cells by Upregulating miR-200c but Downregulating AKT2 Expression. J. Cancer. https://doi.org/10.7150/jca.19858.
Zhou, J., Gasiewicz, T.A., 2003. 3′-methoxy-4′-nitroflavone, a reported aryl hydrocarbon receptor antagonist, enhances Cyp1a1 transcription by a dioxin responsive element-dependent mechanism. Arch. Biochem. Biophys.